Partitioning *in situ* total spectral absorption by use of moored spectral absorption–attenuation meters

Grace C. Chang and Tommy D. Dickey

High-temporal-resolution spectral absorption data were acquired by use of one bottom-mounted (~68-m) and three moored spectral absorption and attenuation meters (ac-9 meters at 14, 37, and 52 m) on the Middle Atlantic Bight continental shelf during the fall 1996 period of the Coastal Mixing and Optics experiment. We employed a previously published spectral absorption model with the data to partition total absorption into absorption by water, phytoplankton, detritus, and gelbstoff (dissolved matter). We validated the model by comparing its results against coincident *in vivo* absorption coefficients derived from discrete bottle samples. Correlations between modeled and *in vivo* spectra range from 0.873 to 0.998. We optimized these correlations to determine the model parameters. These parameters could not be determined solely from the moored ac-9 results. Therefore a separate set of absorption measurements (from discrete bottle samples) was necessary to permit values for the model parameters to be determined. Model results allow us to separate particulate and dissolved components of absorption and to examine the temporal variability and the vertical distributions and concentrations of each component, given the total absorption in the water column.

OCIS code: 010.4450.

1. Introduction

The total absorption coefficient, $a_t(\lambda)$ (expressed in inverse meters), is the fraction of the incident light flux that is absorbed per unit thickness of a sample volume.[1] Whole water absorption is important in determining the magnitude and the spectral shape of the light field in an aquatic medium. In addition, it is a required parameter for solution of the radiative transfer equation (to determine apparent optical properties from the inherent optical properties) for the radiance distribution as a function of depth.[2] It is also important for the interpretation of remote-sensing data, e.g., for obtaining remote-sensing reflectance from inherent optical properties.[3] Therefore it is necessary to determine the absorption coefficient to describe the subsurface radiance distribution.[4]

Furthermore, accurate measurements of phytoplankton absorption are central to bio-optical models of primary productivity,[5] determinations of changing photoecology, and estimations of the role of phytoplankton in heat flux and light attenuation.[6] The presence of detrital and dissolved matter in seawater complicates the direct measurement of phytoplankton absorption. To partition absorption into its four major absorbing components (water, detritus, phytoplankton, and gelbstoff), spectral models have been developed (see, e.g., Roesler *et al.*[7] and Bricaud and Stramski[8]). The development of these models parallels the evolution of optical instruments designed specifically for the measurement of bio-optical parameters (absorption, attenuation, scattering, etc.).

In recent years, spectral absorption and attenuation meters (e.g., ac-3, ac-9, and Hi-Star[9]) have been used in profile mode, providing high vertical resolution absorption and attenuation data during shipboard operations.[10] One advantage of this method is that instruments can be calibrated between successive casts, ensuring accurate measurements over the course of the experiments. However, shipboard profile sampling is usually limited to a few weeks' duration with sampling intervals of hours or greater. An additional disadvantage is that measurements are not taken at time scales short enough to resolve many important higher-frequency oceanographic processes and events (i.e., diel, wind mixing, internal waves, and advection). Long-term variability (seasonal)

The authors are with the Ocean Physics Laboratory, University of California at Santa Barbara, 6487 Calle Real Unit A, Goleta, California 93177. The e-mail address for G. C. Chang is grace@icess.ucsb.edu; for T. D. Dickey it is tommy@icess.ucsb.edu.

Received 8 December 1998; revised manuscript received 13 April 1999.

0003-6935/99/183876-12$15.00/0

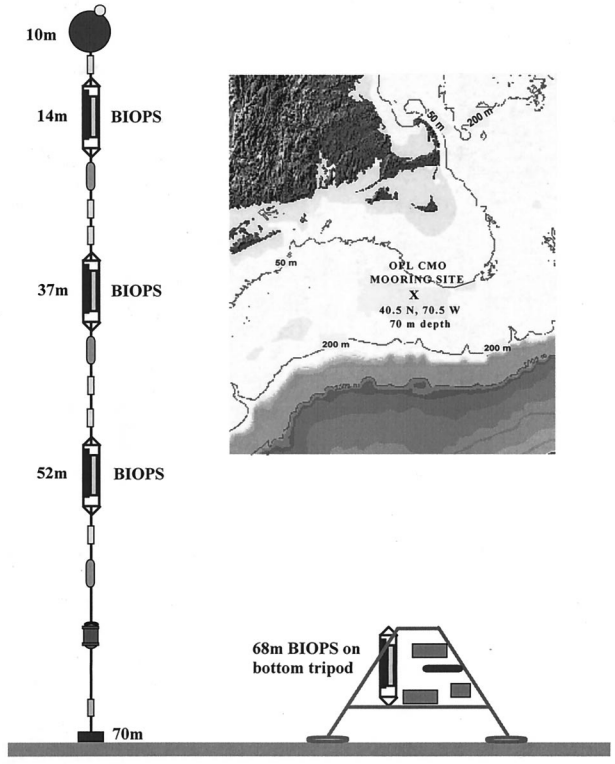

Fig. 1. Geographic map indicating the site of the mooring and tripod used for the present study. Schematic diagrams of mooring and tripod are also shown. OPL, Ocean Physics Laboratory; BIOPS, bio-optical system.

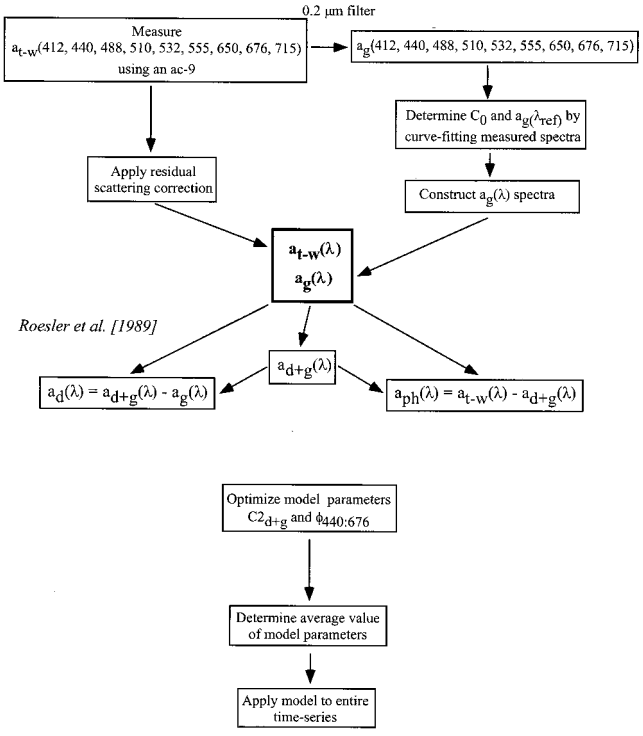

Fig. 2. Flow chart diagramming the procedures used for data analysis, beginning with the measurement of $a_{t-w}(\lambda)$ and $a_g(\lambda)$ with ac-9's (without and with a 0.2-μm filter, respectively). Model inputs and outputs are shown.

and episodic events are also difficult to resolve because of the need for nearly continuous shipboard sampling, which can be precluded by sea-state condition. Moored instruments, on the other hand, can sample every few minutes for months and longer with redeployments and thus can provide information that is relevant to high-frequency and episodic events and long-term variability.[11,12]

We collected high-temporal-resolution spectral absorption and attenuation data, using moored and bottom-mounted ac-9's at discrete depths during the Coastal Mixing and Optics (CMO) experiment (Fig. 1). The CMO experiment was designed for the study of the effect of mixing on inherent and apparent optical properties in the water column. Long-term objectives for the CMO study included partitioning particles by type and relating physical processes to optical variability. We partitioned the high-temporal-resolution spectral absorption measured during the CMO experiment into its four major absorbing components, using the model of Roesler *et al.*,[7] to examine the vertical and temporal variability of particle types throughout the water column. A diagram of the procedures used for data analysis in this study is shown as Fig. 2. Here we present the time-series data set, the results of spectral modeling of these observations, and a brief description of the vertical and temporal variability of water column optical and particle characteristics.

2. Methods

The site of the CMO experiment was the Mud Patch of the Middle Atlantic Bight continental shelf, approximately 110 km south of Martha's Vineyard, Cape Cod, Massachusetts (Fig. 1). The Mud Patch is characterized as a deposit of fine-grained sediment (2–14 m thick) consisting of as much as 95% silt plus clay.[13] High sedimentation rates in the area have been attributed to a decrease in tidal currents over the site.[14] During the first (fall) CMO mooring–tripod deployment, three bio-optical systems were placed upon a subsurface mooring at 14-, 37-, and 52-m depths and a fourth at 2 m above the bottom on a tripod; water depth was approximately 70 m (Fig. 1). The fall deployment of the subsurface mooring extended from 8 July through 26 September 1996. The tripod was deployed from 9 August through 26 September 1996. The bio-optical systems used the following instruments: (1) Biospherical Instruments, Inc., photosynthetically available radiation scalar irradiance sensor (QSP-200; 14, 37, and 52 m), (2) Biospherical Instruments, Inc., upwelling radiance sensor (683 nm; MRP-200; 14 and 37 m), (3) Sea Tech, Inc., fluorometer[15] (52 and 68 m), (4) WET Labs, Inc., WETStar fluorometer (all depths), (5) Sea Tech, Inc., transmissometer[16] (660 nm; all depths), (6) Sea-Bird Electronics, Inc., temperature sensor (SBE 3; all depths), and (7) WETLabs, Inc., ac-9 (Ref. 17; all depths). The sampling rate for the ac-9 was

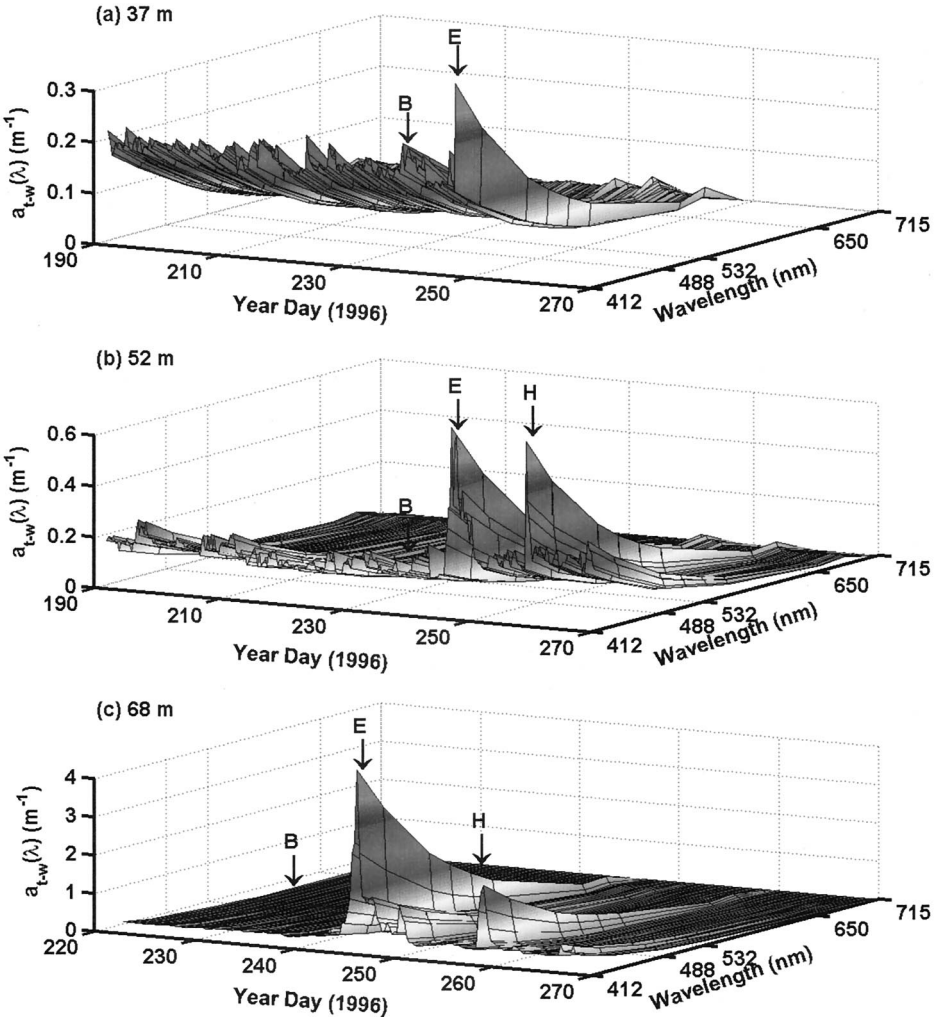

Fig. 3. Time-series (6-h averaged) of total absorption spectra at (a) 37 m, (b) 52 m, and (c) 68 m. B, observed phytoplankton bloom; E, time of passage of Hurricane Edouard; H, time of passage of Hurricane Hortense. Dates are presented as decimal year days, with the convention that 0 h UTC on 1 January is day 1.0.

once per hour, and the sampling rate for all other sensors was once every 7.5 min.

The ac-9 provides concurrent measurements of water absorption and attenuation coefficients at nine wavelengths: λ = 412, 440, 488, 510, 532, 555, 650, 676, and 715 nm with a dual-path optical configuration (see Moore and Bruce[18] for details). WETLabs, Inc., calibrates the ac-9 to provide a zero-point reading for each channel in specially filtered clean, fresh water, using a Millipore Alpha-Q water system. The final output of the ac-9 is the absorption and attenuation coefficients with pure water values (as determined by Smith and Baker[19]) subtracted out [resulting in $a_{t-w}(\lambda)$ and $c_{t-w}(\lambda)$, expressed in inverse meters, where w represents pure water and t is the total spectral absorption]. The accuracy of the ac-9, as reported by WETLabs, Inc., is ± 0.001 m^{-1}. In addition to calibrations, corrections for internal temperature, scattering, and salinity and *in situ* temperature [$a_{t-w}(715)$ only] were applied following the methods described by Moore and Bruce.[18] Absorption at the 715-nm wavelength was subtracted from the entire spectrum to correct for residual light scattering. This zero-scattering correction was performed to conform to discrete bottle sample methods of obtaining absorption spectra (see below). This correction is an approximation and is a possible source of error (see Section below).

In vivo total (without water), phytoplankton, detrital, and gelbstoff absorption data derived from discrete bottle samples were provided by Heidi Sosik (Woods Hole Oceanographic Institution) and Collin Roesler (University of Connecticut) for comparison with modeled values. These discrete bottle samples were obtained approximately daily by Roesler during the fall CMO cruise over the period 17 August–7 September 1996. Depths of bottle samples varied from ~1 m (just below the water's surface) to 60 m. Only data sampled within 3 m of the mooring depths were used in this analysis. Data from 21 and 31 August 1996 at a depth of 37 m and 21 and 25 August 1996 at a depth of 52 m are presented for this study. For the soluble absorption (gelbstoff) a water sample was filtered through prerinsed 0.2-μm polycarbonate

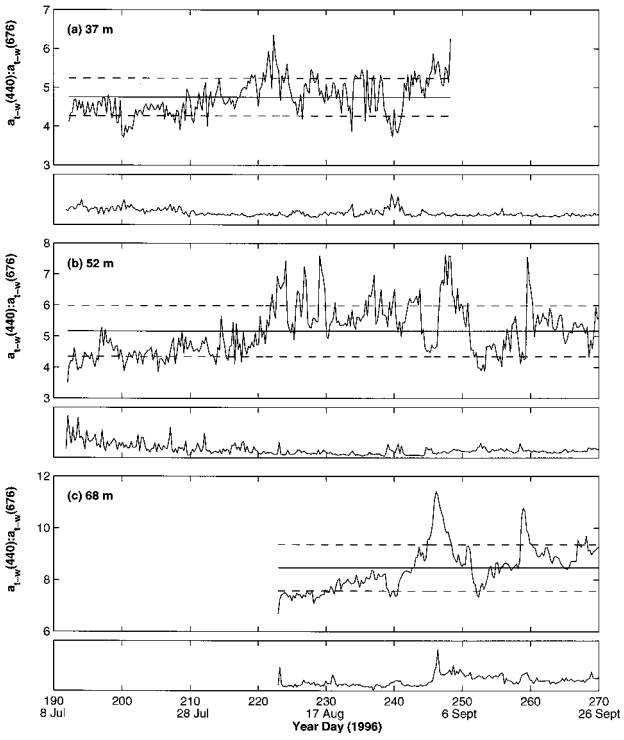

Fig. 4. Time series of the ratio $a_{t-w}(440):a_{t-w}(676)$ (6-h-averaged) and chlorophyll-a concentrations derived from the WET-Star fluorometer plotted with an arbitrary scale (beneath ratio time series) at (a) 37 m, (b) 52 m, and (c) 68 m. Note the change in scales of the ordinate axes. Solid horizontal lines, means of the time series; dashed horizontal lines, one standard deviation from the mean. Dates are presented as decimal year days, with the convention that 0 h UTC on 1 January is day 1.0.

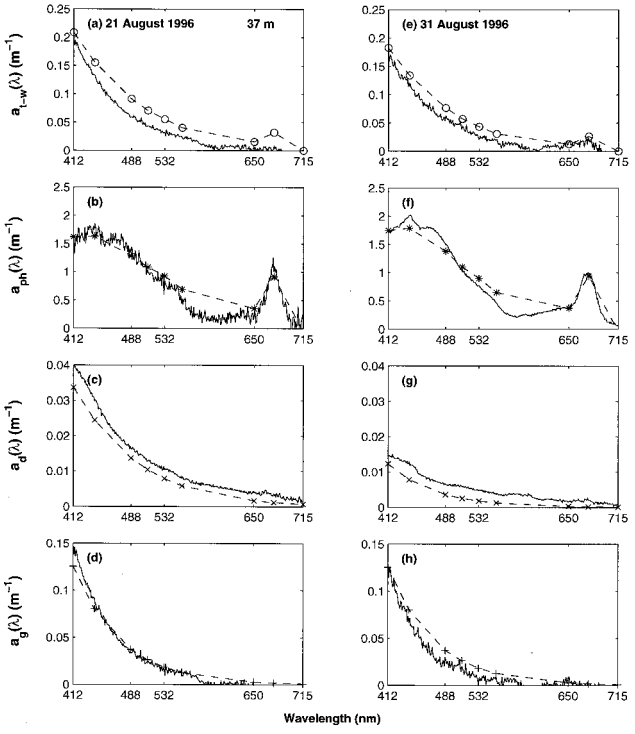

Fig. 5. *In vivo* bottle sample measured (solid curves) and ac-9-derived (dashed curves): (a) total absorption spectra without water, (b) phytoplankton absorption normalized to the 676-nm wavelength, (c) detrital absorption, (d) gelbstoff absorption for 21 August 1996 (year day 234); (e) total absorption without water, (f) phytoplankton absorption normalized to the 676-nm wavelength, (g) detrital absorption, (h) gelbstoff absorption for 31 August 1996 (year day 244) from the model of Roesler *et al.*[7] at the 37-m depth.

filters and the filtrate was stored at 4 °C. Gelbstoff absorption spectra were then measured in 10-cm quartz cuvettes with Milli-Q water in the reference beam. Particles were collected on glass fiber filters and analyzed in accordance with the guidelines specified by Mitchell.[20] Particulate absorption spectra were measured with a Perkin-Elmer Lambda 18 dual-beam UV–visible spectrophotometer with a 60-μm integrating sphere. Following pigment extraction in hot methanol,[21] pad absorption was remeasured, yielding values of detrital absorption. Absorption by phytoplankton pigments was estimated as the difference between total particulate and detrital absorption values. We used the Mitchell[20] beta algorithm to estimate absolute absorption coefficients from raw optical density. For each spectrum, average values for wavelengths of 780–800 nm for particulate samples and of 660–670 nm for soluble samples were subtracted from the entire spectrum to correct for residual light scattering. This zero correction for scattering is an approximation, and the choice of wavelength range is somewhat subjective.[22]

3. Observations

We recovered 80- and 50-day time-series data sets from the 52- and 68-m ac-9's, respectively [Figs. 3(b) and 3(c)]. The 37-m ac-9 was biofouled shortly after the passage of Hurricane Edouard[23] on 6 September 1996, providing us with 60 days of data [Fig. 3(a)]. The 14-m ac-9 data began to show the effects of biofouling (exponential growth of the absorption and attenuation signals) approximately 15 days after the instrument was deployed and hence were not used in this study. W. Scott Pegau (Oregon State University) intercompared all nonbiofouled data with available shipboard ac-9 profile measurements to determine possible errors from long-term instrument drift. Results from the intercomparisons revealed that instrument drift was small, with differences of approximately ±15% between moored and profiled data, which was within the variability of the tidal signal. Data from the 37-, 52-, and 68-m ac-9 time series were used with the spectral absorption model mentioned above.

A. 37-m ac-9 Data

A three-dimensional plot of 37-m ac-9 total absorption spectra $[a_{t-w}(\lambda)]$ over the available time series (8 July–6 September 1996; year days 190–250, with the convention that 0 h UTC on 1 January is day 1.0), with a 6-h average (for a clearer depiction of the data), is shown in Fig. 3(a). The 37-m spectra and wavelength ratio (440:676 nm; Figs. 3 and 4) show a

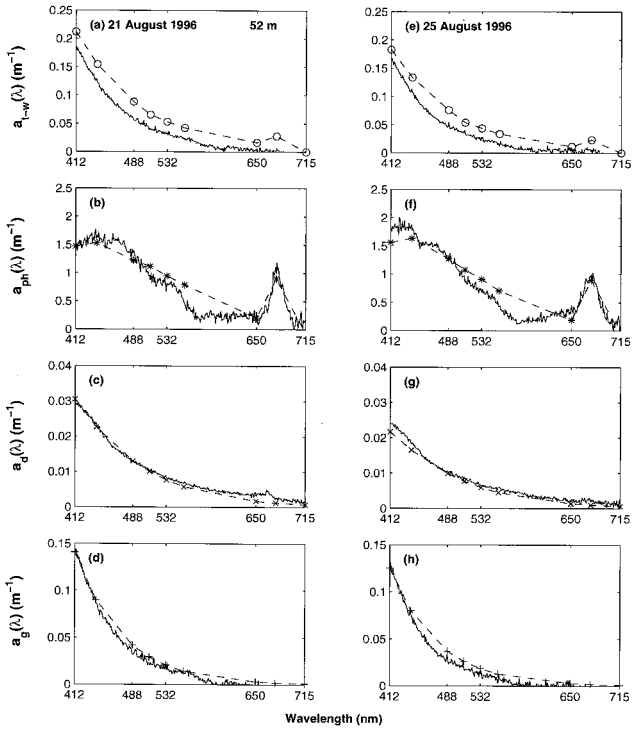

Fig. 6. *In vivo* bottle sample measured (solid curves) and ac-9-derived (dashed curves): (a) total absorption spectra without water, (b) phytoplankton absorption normalized to the 676-nm wavelength, (c) detrital absorption, (d) gelbstoff absorption for 21 August 1996 (year day 234); (e) total absorption without water, (f) phytoplankton absorption normalized to the 676-nm wavelength, (g) detrital absorption, (h) gelbstoff absorption for 25 August 1996 (year day 238) from the model of Roesler *et al.*[7] at the 52-m depth.

strong phytoplankton signature, which can be seen in the chlorophyll-*a* red absorption peak (676 nm). The spectral shape, however, was not constant throughout the time series. This fact is demonstrated in a time-series plot of the ratio $a_{t-w}(440)$:$a_{t-w}(676)$ [6-h average; Fig. 4(a); chlorophyll-*a* concentration time series with an arbitrary scale shown below each absorption ratio time series for comparison]. This ratio ranged from 3.5 to 6.5 from 8 July through 6 September 1996. The relatively low ratio signifies a higher amount of chlorophyll-*a* at 37 m than at 52 and 68 m. During most of the 60-day time series the ratio was within one standard deviation of the mean [Fig. 4(a)]. However, several significant changes in the spectral shape occurred on 18 July, 7 August, 26 August, and 1 September 1996. The ratio $a_{t-w}(440)$:$a_{t-w}(676)$ decreased on 18 July and 26 August 1996; i.e., chlorophyll-*a* concentration increased relative to those of other constituents [Fig. 4(a)]. These changes were most likely the result of relatively small-scale and short-lived phytoplankton blooms.[24] Fluorescence profiles obtained by Pegau on 26 August 1996 show a greater than threefold increase in chlorophyll-*a* centered at the 30-m depth, lasting for ~3 days [data not shown; peak B in Fig. 3(a)]. The increases in the ratio $a_{t-w}(440)$:$a_{t-w}(676)$ on 7 August and 1 September 1996 were most likely caused by horizontal advection of different water masses past the CMO site or by resuspension of bottom sediments. The high ratio of $a_{t-w}(440)$:$a_{t-w}(676)$ on 4 September 1996 [peak E in Fig. 3(a)] was due to the passage of Hurricane Edouard over the CMO site, which forced bottom sediment more than 30 m upward into the water column.[23] The higher-frequency oscillations seen in the time series of $a_{t-w}(440)$ to $a_{t-w}(676)$ at all depths were due to the diel cycle (Fig. 4).

B. 52-m ac-9 Data

The signature of the 52-m ac-9 spectral time series [6-h average; Fig. 3(b)] was significantly different from that of the 37-m data. It is worth noting that there is little indication of vertical settling through the water column, most likely because of high horizontal advection at the CMO site. The spectral shape varied greatly throughout much of the time series, with large increases in magnitude during the passage of two hurricanes, Edouard [3 September 1996; year day 247; peak E in Fig. 3(b)] and Hortense [15 September 1996; year day 259; peak H in Fig. 3(b)]. The higher $a_{t-w}(440)$:$a_{t-w}(676)$ ratio indicates lower concentrations of chlorophyll-*a* at the 52-m than at the 37-m depth. This result was expected because of the proximity to the ocean bottom (<20 m) and the decreased light levels at this depth (1% light level was at ~35 m; data not shown). Similarly to that in the 37-m time-series, the ratio $a_{t-w}(440)$:$a_{t-w}(676)$ generally remained within one standard deviation of the mean, except during periods of high sediment resuspension (3 and 15 September 1996) and horizontal advection.

Table 1. Model Parameters and Regression Results Derived from the Spectral Model of Roesler *et al.*[a]

Day (August 1996)	Depth (m)[b]	$C2_{d+g}$ (nm^{-1})	$\phi_{440:676}$	r^2 (ph)[c]	r^2 (d)[c]	r^2 (g)[c]
21	38	0.015	1.60	0.979	0.988	0.998
	53	0.015	1.50	0.881	0.997	0.996
25	55	0.015	1.90	0.873	0.997	0.996
31	36	0.016	1.75	0.942	0.932	0.972

Regression analysis was performed between partitioned *in situ* ac-9 data and *in vivo* validation absorption spectra for the 37-m depth on 21 and 31 August 1996 and for the 52-m depth on 21 and 25 August 1996 for all ac-9 wavelengths except 715 nm.

[a]Ref. 7.

[b]Depths of discrete bottle samples, chosen within 3 m of the mooring depths (37 and 52 m).

[c]ph, Phytoplankton; d, detrital; g, gelbstoff.

C. 68-m ac-9 Data

The 68-m spectral absorption time series [6-h average; Fig. 3(c)] can be described in two parts: before the passage of the two hurricanes (prehurricane; 7–29 August 1996; year days 220–242) and during the passage of the hurricanes[23] (30 August–26 September 1996; year days 243–270). During prehurricane conditions the spectra were similar in shape to the 37-m data, although the large concentration of detritus at the near-bottom depth (68 m) increased the ratio $a_{t-w}(440)$:$a_{t-w}(676)$ [Fig. 3(c) and 4(c)]. Chlorophyll-a absorption peaks are detectable at the red wavelength (676 nm), possibly because of resuspension of relict pigments from the ocean bottom, sinking of phytoplankton, or both. This phenomenon is difficult to see in Fig. 3(c) because of the scale of the absorption axis. During the hurricanes, the magnitude of total absorption and the ratio $a_{t-w}(440)$:$a_{t-w}(676)$ increased dramatically owing to resuspended bottom sediments. The absorption spectra increased exponentially with increasing wavelength during this time.

4. Analyses

Our analysis procedure to partition total absorption measured by the ac-9 (without water) into absorption by phytoplankton, detritus, and gelbstoff is summarized in Fig. 2. The total spectral absorption, $a_t(\lambda)$, can be described as the sum of spectral absorption that is due to water, $a_w(\lambda)$; to phytoplankton, $a_{\mathrm{ph}}(\lambda)$; to detritus, $a_d(\lambda)$; and to gelbstoff, $a_g(\lambda)$, such that

$$a_t(\lambda) = a_w(\lambda) + a_{\mathrm{ph}}(\lambda) + a_d(\lambda) + a_g(\lambda). \quad (1)$$

The absorption spectrum for water is known.[19,25] The shape and magnitude of the detritus and gelbstoff spectra can be modeled with minimal error.[1,26] However, phytoplankton spectral absorption varies significantly in response to environmental changes and community composition. Thus one generally derives phytoplankton absorption signatures from whole-water absorption measurements by first subtracting other, less variable, absorption components (water, detritus, gelbstoff).

Gelbstoff absorption spectra have been successfully modeled with a simple exponential function[26]:

$$a_g(\lambda) = a_g(\lambda_{\mathrm{ref}}) \exp[-C_0(\lambda - \lambda_{\mathrm{ref}})], \quad (2)$$

where λ_{ref} is a reference wavelength (λ_{ref} was chosen to be 440 nm for this study) and C_0 is a constant (expressed in inverse nanometers). Gelbstoff spectra for the CMO study were measured by Pegau ~3 times daily during the period 17 August–7 September 1996; he used shipboard profiling methods with a 0.2-μm filter on the intake of an ac-9 absorption tube. Therefore gelbstoff absorption is defined for the purpose of this study as any particle that passes through a 0.2-μm filter. The shape and magnitude of the gelbstoff spectra remained relatively constant with depth and time before the passage of Hurricane Edouard.[24] C_0 was estimated to be 0.016 ± 0.001 nm^{-1}, and a value for $a_g(440)$ was estimated to be 0.08 m^{-1} based on curve fitting of all ac-9 measured gelbstoff spectra.[24]

The model of Roesler *et al.*[7] does not distinguish between detrital absorption and gelbstoff absorption spectra. The model was developed for high-chlorophyll coastal waters but can also be used for case I waters (for which phytoplankton determine the optical properties in the water column)[1] with appropriate determination of model parameters:

$$a_{d+g}(\lambda) = \{a_{d+g}(\lambda_{\mathrm{ref}}) \exp[C2_{d+g}(\lambda_{\mathrm{ref}} - 400)]\}\exp[-C2_{d+g}(\lambda - 400)], \quad (3)$$

where $C2_{d+g}$ (expressed in inverse nanometers) is an unknown model parameter that defines the shape of the detritus-plus-gelbstoff spectra and $a_{d+g}(\lambda_{\mathrm{ref}})$ is an unknown absorption for the detritus-plus-gelbstoff spectra at a reference wavelength. The value of $C2_{d+g}$ is estimated from measurements at the specific site (average values are 0.011–0.016 nm^{-1}) and is influenced by the relative contributions of humic or fulvic acid. $a_{d+g}(\lambda_{\mathrm{ref}})$ can be determined under the assumption of Kishino *et al.*[21] that total absorption at 676 nm is due mainly to absorption of phytoplankton, with minimal or no contribution from gelbstoff or detritus absorption. Assuming that $a_{d+g}(676)$ is negligible compared with $a_{\mathrm{ph}}(676)$, we obtained the following relationship[7]:

$$a_{d+g}(440) = a_{t-w}(440) - a_{t-w}(676)\phi_{440:676}, \quad (4)$$

where $a_{d+g}(440)$ represents $a_{d+g}(\lambda_{\mathrm{ref}})$ in Eq. (3) at a reference wavelength of 440 nm, $a_{t-w}(\lambda)$ is the total absorption minus the contribution of water, and $\phi_{440:676}$ is the measured blue-to-red absorption peak ratio for phytoplankton. $\phi_{440:676}$ depends on water type, species type, light history, nutrients, pigment composition, and pigment packaging effects.[7] Absorption that was due to the presence phytoplankton was determined with the following relationship from total absorption data obtained during the CMO experiment (case II waters, in which resuspended sediment or dissolved or colored matter dominates the optical properties of the water column)[1]:

$$a_{\mathrm{ph}}(\lambda) = a_{t-w}(\lambda) - a_{d+g}(\lambda), \quad (5)$$

where $a_{t-w}(\lambda)$ is measured by the ac-9 and $a_{d+g}(\lambda)$ is determined from Eq. (3).

Detrital absorption was determined by the difference

$$a_d(\lambda) = a_{d+g}(\lambda) - a_g(\lambda). \quad (6)$$

Details of the methods and model development are described by Roesler *et al.*[7]

The partitioning of total absorption spectra into absorption by phytoplankton, detritus, and gelbstoff was performed with the model of Roesler *et al.*[7] described above for days when validation *in vivo* absorption data were available at depths within 3 m of the ac-9 mooring measurements. We applied the model of Roesler *et al.*[7] to the total absorption spectra at 37 m for 21 and 31 August 1996 and at 52 m for 21

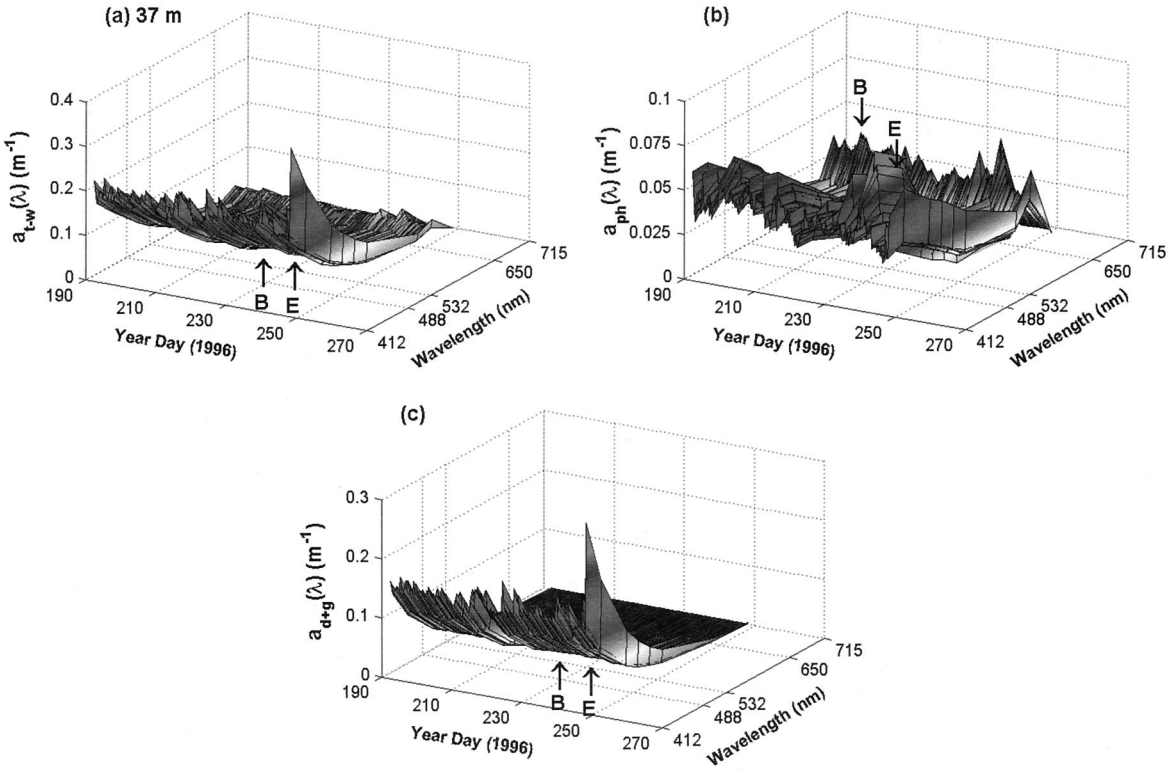

Fig. 7. Time series (6-h average) of 37-m (a) total absorption spectra (without water) measured by the ac-9, (b) phytoplankton absorption spectra, and (c) detrital-plus-gelbstoff absorption estimated from the model of Roesler *et al.*[7] B, timing of a phytoplankton bloom; E, time of passage of Hurricane Edouard. Dates are presented as decimal year days, with the convention that 0 h UTC on 1 January is day 1.0.

and 25 August 1996 at exact times of discrete bottle sample collection to partition $a_{t-w}(\lambda)$ into $a_{\mathrm{ph}}(\lambda)$, $a_d(\lambda)$, and $a_g(\lambda)$. The gelbstoff absorption spectra were computed from Eq. (2) with the assumption that $C_0 = 0.016\ \mathrm{nm}^{-1}$ and $a_g(440) = 0.08\ \mathrm{m}^{-1}$ for 21 and 31 August 1996 and at 52 m for 21 and 25 August 1996 at times of discrete bottle sample collection.[24] Total and partitioned absorption spectra measured by the ac-9 and determined from the model were then compared with total, phytoplankton, detritus, and gelbstoff absorption spectra measured with the *in vivo* absorption data. Figures 5 and 6 show modeled and measured absorption spectra at 37- and 52-m depths, respectively (phytoplankton absorption spectra shown have been normalized to the 676-nm wavelength). Parameters used for the model of Roesler *et al.*[7] are found in Table 1. We optimized the estimates with that model by varying the model parameter $C2_{d+g}$ from 0.011 to 0.016 nm^{-1} in steps of 0.001 nm^{-1} and by varying $\phi_{440:676}$ from 1.0 to 2.0 in steps of 0.1 to yield the best correlations. After the optimizations were performed, average values for the constants $C2_{d+g}$ and $\phi_{440:676}$ were computed and applied to the entire 37- and 52-m ac-9 time-series data (8 July–6 September 1996 and 8 July–26 September 1996, respectively) for estimates of $a_{\mathrm{ph}}(\lambda)$ and $a_{d+g}(\lambda)$. The results are shown in Figs. 7 and 8. We estimated model constants for 68-m absorption data by varying $C2_{d+g}$ and $\phi_{440:676}$ until the shapes of $a_{\mathrm{ph}}(\lambda)$ and $a_{d+g}(\lambda)$ simultaneously appeared to be consistent with published partitioned absorption spectra at all time periods.[7,8,27] These model constants were then applied to the entire 68-m total absorption time-series data (50 days; Fig. 9).

5. Results and Discussion

Regression analysis was performed between partitioned *in situ* ac-9 data (modeled) and *in vivo* validation absorption spectra (measured) for the 37-m depth on 21 and 31 August 1996 and for the 52-m depth on 21 and 25 August 1996 (Table 1) for all ac-9 wavelengths with the exception of 715 nm. The 715-nm wavelength was excluded because of its variability associated with changes in temperature and salinity.[18,28,29] High correlation was found between modeled and measured phytoplankton, detritus, and gelbstoff spectral shapes at 37- and 52-m depths (Table 1). The phytoplankton spectra consistently yielded the lowest correlation (0.873–0.979), and the gelbstoff spectra yielded the highest (0.972–0.998). Detritus spectra correlation ranged from 0.932 to 0.997. These rates of correlation were to be expected because gelbstoff and detritus spectra are relatively well known and easily modeled, whereas phytoplankton spectra vary according to phytoplankton concentration, community structure, and physiology as well as changes in pigment composition and packaging.[7,30]

As much as 27% error associated with the prediction of phytoplankton absorption spectral shapes was reported for the data presented by Roesler *et al.*[7]

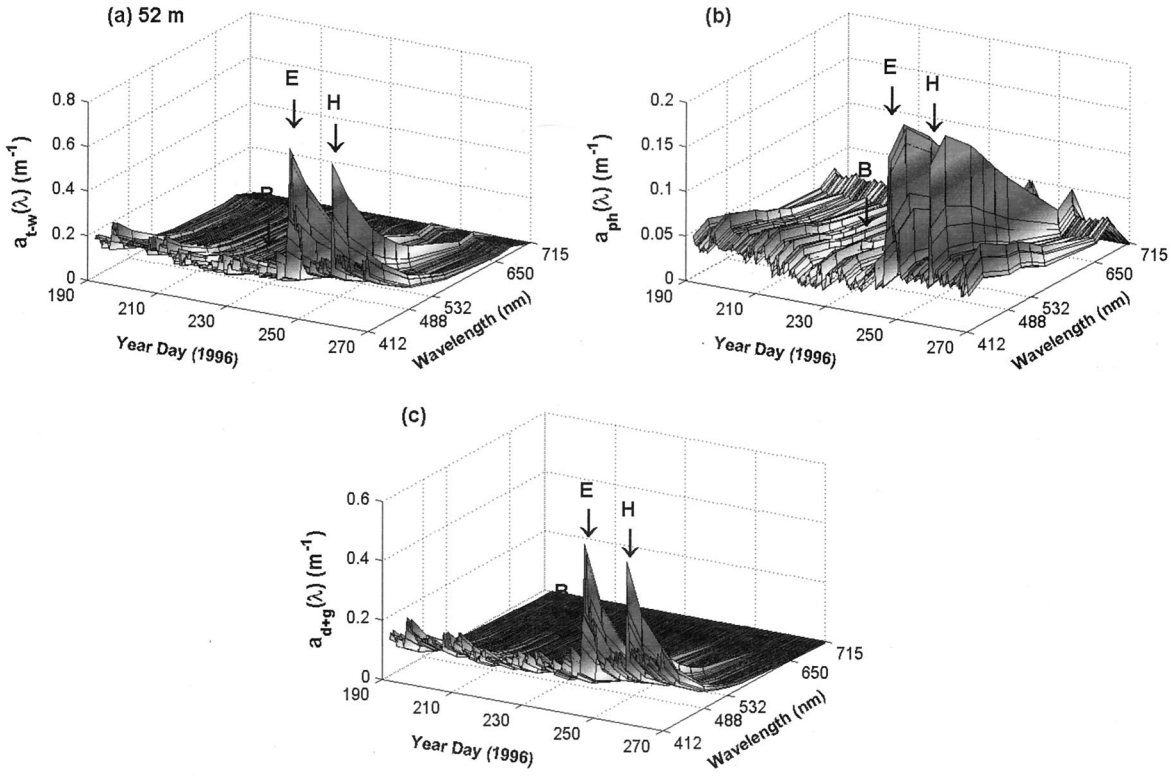

Fig. 8. Time series (6-h average) of 52-m (a) total absorption spectra (without water) measured by the ac-9, (b) phytoplankton absorption spectra, and (c) detrital-plus-gelbstoff absorption estimated from the model of Roesler *et al.*[7] B, timing of a phytoplankton bloom; E, time of passage of Hurricane Edouard; H, time of passage of Hurricane Hortense. Dates are presented as decimal year days, with the convention that 0 h UTC on 1 January is day 1.0.

Table 2 shows average percent differences between modeled and measured phytoplankton, detrital, and gelbstoff absorption for the model of Roesler *et al.*[7] for all wavelengths except 715 nm. The differences between modeled and measured results from this study can be attributed to bottle sample analyses, ac-9 measurements, model assumptions, and determination of model parameters. The high percent differences in the blue and red wavelengths (412, 440, 650, and 676 nm) of the phytoplankton and detrital absorption are possibly due to residual pigments that were not removed from detrital spectra during determination of the *in vivo* spectra. Evidence for this can be seen in the slight peaks at 440 and 676 nm of the *in vivo* detrital curves (Figs. 5 and 6). The methanol extraction technique used to determine absorption by phytoplankton may have generated additional measurement error in that it may have included absorption by nonphotosynthetic carotenoids and detrital pigments,[7] thus overestimating phytoplankton absorption. Variations in the optical properties of the filter pads used in the analysis of bottle sample data could also have led to inaccurate measurements of absorption.[31] Large errors in the measurement of the red wavelengths of gelbstoff absorption can be attributed to the zero correction for scattering. Calibration errors of the ac-9's may have also affected the total absorption spectral shape used as inputs into the model. The model parameter $C2_{d+g}$ and $\phi_{440:676}$ greatly affected the model results. Varying $C2_{d+g}$ and $\phi_{440:676}$ for the model of Roesler *et al.*[7] resulted in a change in the correlation from 0.197 to 0.979 for 21 August 1996 (data not shown).

It should be noted that slight magnitude differences between *in situ* and *in vivo* $a_{t-w}(\lambda)$ (Fig. 5 and 6) exist. *In situ* $a_{t-w}(\lambda)$ measured by the ac-9 was consistently greater than *in vivo* $a_{t-w}(\lambda)$, most likely because of the arbitrary wavelength selection for the zero correction for scattering. Bottle sample–derived total absorption data drop below zero at ~680 nm, which is the peak in chlorophyll-*a* absorption (Fig. 5), providing evidence that the *in vivo* total absorption is too low. An additional reason for these differences may be dissimilar sampling schemes. The sample volumes measured by the moored instruments and the bottle samples were not obtained from the same water mass, and there is clearly considerable spatial variability (horizontal and vertical) in the region.[32] Evidence for this difference can be found in ac-9 profile data taken by Pegau (data not shown). Great variations can be found in profile absorption data over several casts at one location. These variations may have been due to internal waves, advection, or measurement errors. Slight variations in sampling depth (e.g., 35 versus 37 m or 50 versus 52 m) may have also contributed to the differences in magnitude.

The use of the spectral model presented by Roesler *et*

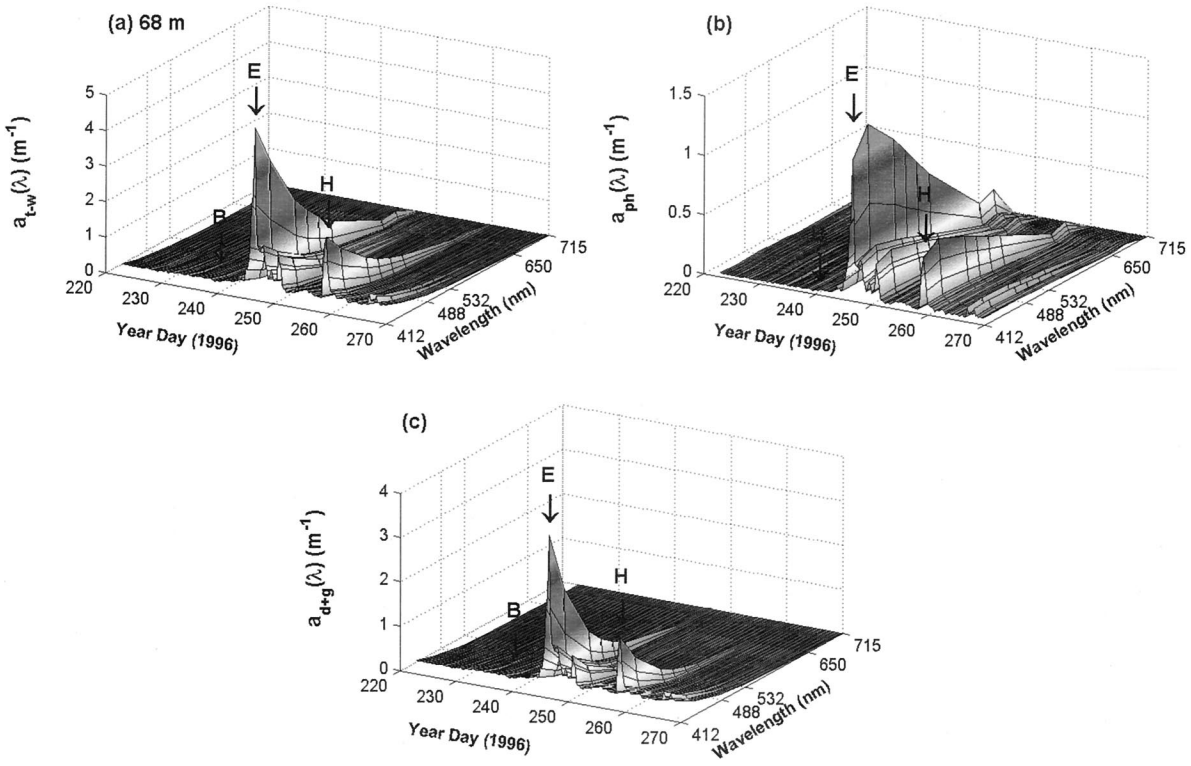

Fig. 9. Time series (6-h average) of 68-m (a) total absorption spectra (without water) measured by the ac-9, (b) phytoplankton absorption spectra, and (c) detrital-plus-gelbstoff absorption estimated from the model of Roesler *et al.*[7] B, timing of a phytoplankton bloom; E, time of passage of Hurricane Edouard; H, time of passage of Hurricane Hortense. Dates are presented as decimal year days, with the convention that 0 h UTC on 1 January is day 1.0.

al.[7] to partition total absorption for the entire time series at 37-, 52-, and 68-m depths at the CMO site allowed us to determine particle types and the relative concentration of each type, given total absorption in the water column (Figs. 7–9; 6-h averages shown). Average total and partitioned absorption, and percent contribution of partitioned to total absorption at the 412 nm wavelength, are listed in Table 3. Before use of the spectral partitioning model, analysis of absorption data revealed only that higher-absorbing materials were present at the bottom (68 m) than at the top (37 m) and the middle (52 m) of the water column.

The results from this model reveal the vertical structure of absorption by phytoplankton, detritus, and gelbstoff. The contribution of phytoplankton to total absorption was highest at 37 m, which was near the depth of the chlorophyll maximum (25–35 m), determined from profiles of chlorophyll fluorescence (Oregon State University data; not shown). Relative phytoplankton absorption decreased with increasing depth, to a minimum of 15.0% of total absorption at 68 m, which was well below the euphotic depth (1% light level; ~35 m). Gelbstoff contribution to total absorption decreased from the top to the bottom of the water column as well. It is hypothesized that the source of dissolved matter at the CMO site was mainly land-derived processes (river runoff, continental weathering) because of the site's close proximity to the

Table 2. Average Percent Difference between Modeled and Measured Absorption for the Spectral Model of Roesler *et al.*[7] throughout All Depths and Time Periods

Wavelength (nm)	$a_{\mathrm{ph}}(\lambda)$ (%)[a]	$a_d(\lambda)$ (%)[a]	$a_g(\lambda)$ (%)[a]
412	+43.6	+20.3	−15.0
440	+48.2	+10.7	−8.6
488	+7.4	+9.2	+0.6
510	−11.1	+3.1	+11.9
532	−21.0	−3.4	+12.5
555	−37.3	−10.0	−0.4
650	−78.3	−51.4	−213.7
676	−24.7	−56.6	−125.5

[a]ph, Phytoplankton; d, detrital; g, gelbstoff.

Table 3. Average Total and Partitioned Absorption and Percent Contribution to Total Absorption at the 412-nm wavelength at 37-, 52-, and 68-m Depth Derived from the Spectral Model of Roesler *et al.* Averaged over the Available Time Series at Each Depth

Absorption (m^{-1})[a]	Depth		
	37 m	52 m	68 m
$a_{t-w}(412)$	0.2013 (100%)	0.2297 (100%)	0.5965 (100%)
$a_{\mathrm{ph}}(412)$	0.0456 (22.7%)	0.0413 (18.0%)	0.0897 (15.0%)
$a_d(412)$	0.0305 (15.2%)	0.0633 (27.6%)	0.3817 (64.0%)
$a_g(412)$	0.1252 (62.2%)	0.1252 (54.5%)	0.1252 (21.0%)

[a]$t - w$, total without water; ph, phytoplankton; d, detrital, g, gelbstoff.

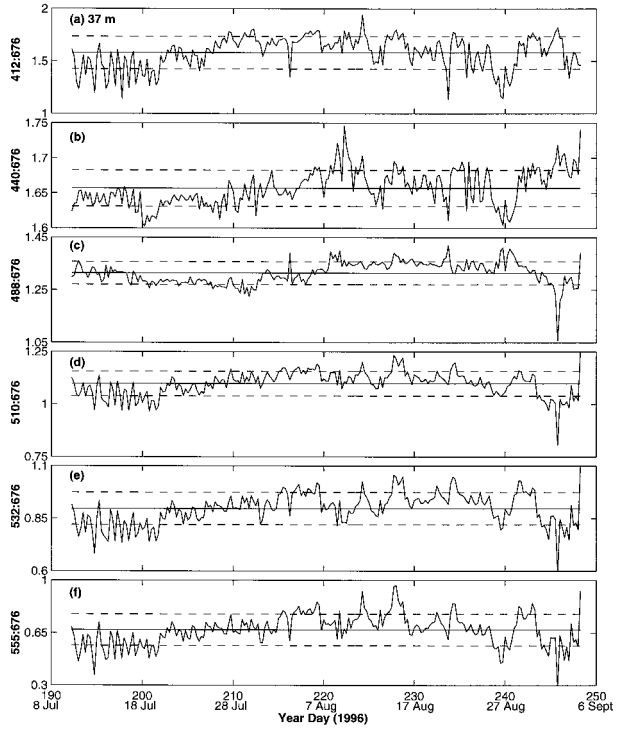

Fig. 10. Time series of 6-h averaged (a) $a_{ph}(412):a_{ph}(676)$, (b) $a_{ph}(440):a_{ph}(676)$, (c) $a_{ph}(488):a_{ph}(676)$, (d) $a_{ph}(510):a_{ph}(676)$, (e) $a_{ph}(532):a_{ph}(676)$, and (f) $a_{ph}(555):a_{ph}(676)$ at the 37-m depth estimated from the model of Roesler *et al*. Solid horizontal lines, means of the time series; dashed horizontal lines, one standard deviation from the mean. Dates also presented as decimal year days, with the convention that 0 h UTC on 1 January is day 1.0.

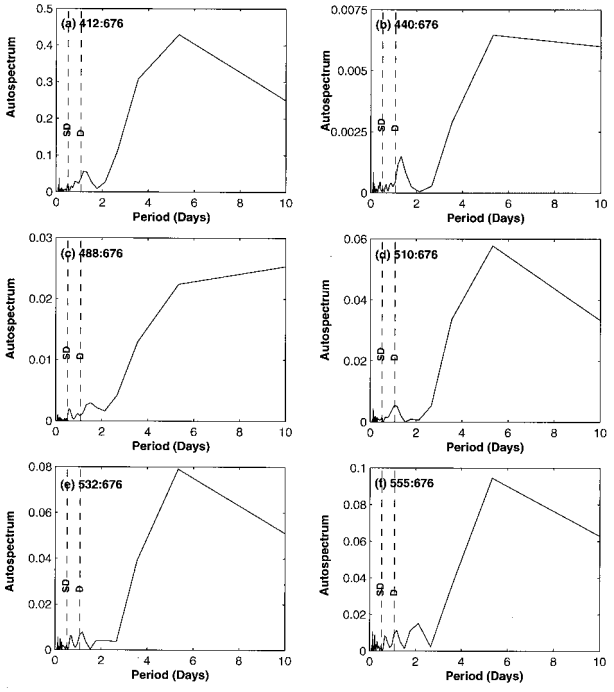

Fig. 11. Frequency autospectra for 6-h-averaged (a) $a_{ph}(412):a_{ph}(676)$, (b) $a_{ph}(440):a_{ph}(676)$, (c) $a_{ph}(488):a_{ph}(676)$, (d) $a_{ph}(510):a_{ph}(676)$, (e) $a_{ph}(532):a_{ph}(676)$, and (f) $a_{ph}(555):a_{ph}(676)$ at the 37-m depth estimated from the model of Roesler *et al*. The dashed vertical lines labeled SD indicate a semi-diurnal tidal period (0.52 day; 12.42 h), and the dashed vertical lines labeled D indicate a diel period (1 day).

coast.[1] Biological productivity at the site (exudation, excretion, microbial autolysis, etc.) may also have had an influence on the gelbstoff distribution. The contribution of detrital matter to total absorption was greatest at the deepest depth (68 m), decreasing toward the top of the water column. This result was not unexpected because of the influence of high concentrations of sediment resuspended from the ocean bottom through tides, currents, and waves.

A. 37-m Partitioned Absorption Time Series

The phytoplankton absorption spectral shape at 37 m was variable with time before 2 September 1996 when Hurricane Edouard passed over the mooring (Fig. 7). The phytoplankton absorption spectra exhibited a shape similar to that of the specific absorption coefficient of chlorophyll-*a*, with peaks in absorption at the blue and red (440- and 676-nm) wavelengths [Fig. 7(a)].[27] The time series of the phytoplankton absorption wavelength ratios (all divided by the 676-nm wavelength; Fig. 10) were different at all wavelengths, representing fluctuations in the spectral shape of phytoplankton absorption over time. The high-frequency variations may have been caused by changes in photoecology (photoadaptations, pigment packaging, etc.). Lower-frequency oscillations may have been due to changes in phytoplankton concentrations, species composition, or both, induced by changing light or nutrient conditions or by advection of new populations past the CMO site. Frequency autospectra were constructed for wavelength ratios (all divided by 676 nm) over the period 8 July–6 September 1996 by use of 256-point fast Fourier transforms, Hanning windows, and zero overlap to determine the dominant periods in the time-series records (Fig. 11). The dominant period at all wavelength ratios was ~5 days, which is approximately the period of community (large-scale) phytoplankton physiological adaptation (3–5 days).[33] These large-scale adaptations were most likely induced by mixing and advection events.[32] Smaller peaks in the frequency autospectra were observed at the semidiurnal tidal period (0.52 day) and the diel period (1 day). Detrital and gelbstoff spectra remained relatively constant with time throughout the entire time series (Fig. 7).

During a phytoplankton bloom on 26 August 1996 (year day 239; peak B in Fig. 7), which lasted approximately 3 days, total absorption increased by ~0.2 m^{-1}. Phytoplankton absorption at 488-, 510-, 532-, and 676-nm wavelengths increased relative to that at all other wavelengths during this time. The phytoplankton absorption spectra during the bloom are similar in shape to diatom absorption spectra (Fig. 12 and Ref. 1). Previous studies showed that the diatom species *Rhizosolenia alata* dominates the Middle Atlantic Bight continental shelf and slope waters

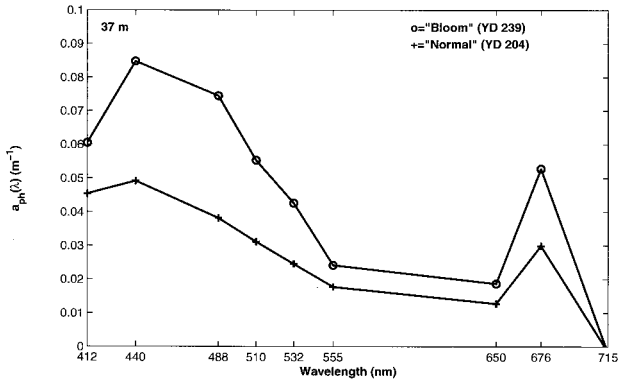

Fig. 12. Phytoplankton absorption spectra partitioned from total absorption at 37 m from the model of Roesler *et al*. on 26 August 1996 [year day (YD) 239] during a phytoplankton bloom and 22 July 1996 (year day 204) during nonbloom conditions.

during the late summer months.[34] Therefore the increase in absorption on 26 August 1996 can be attributed to a diatom bloom.

B. 52- and 68-m Partitioned Absorption Time Series

Phytoplankton absorption spectra at 52 and 68 m exhibited shapes similar to those of the spectra of the specific absorption coefficient of chlorophyll-*a* throughout the period before the passage of Hurricanes Edouard and Hortense (1 and 14 September 1996; Figures 8, 9, and 13), although the relative contribution of phytoplankton to total absorption was lower at these depths. Frequency autospectra of wavelength ratios were similar to those at the 37-m depth (data not shown), with a dominant period of ~5 days. The phytoplankton bloom on 26 August 1996 at 37 m did not affect absorption values at 52 or 68 m. All components of absorption (total, phytoplankton, and detrital plus gelbstoff) increased dramatically during the hurricanes at 52 and 68 m, with a greater increase seen in the blue wavelengths of detritus-plus-gelbstoff absorption (Figs. 4, 8, 9, and 13). Resuspension of detrital pigments and downward mixing of phytoplankton most likely caused the increase of phytoplankton absorption during the hurricanes (Fig. 13).[23]

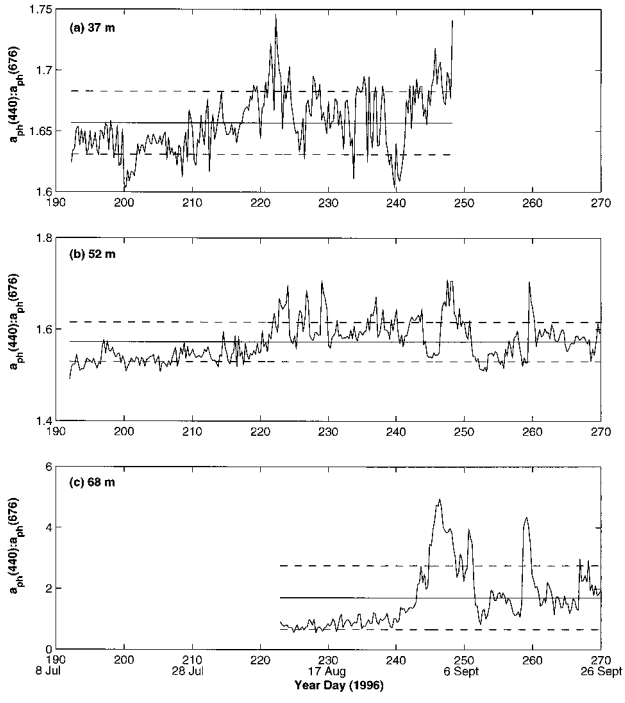

Fig. 13. Time series of the ratio $a_{ph}(440):a_{ph}(676)$ estimated from the model of Roesler *et al*. at the depths shown. Note the change in the scales of the ordinate axes. Solid horizontal lines, means of the time series; dashed horizontal lines, one standard deviation from the mean. Dates are presented as decimal year days, with the convention that 0 h UTC on 1 January is day 1.0.

6. Conclusions

High-temporal-resolution spectral absorption data measured with moored and bottom-mounted spectral absorption and attenuation meters (ac-9's) during the fall deployment of the Coastal Mixing and Optics experiment were used with a spectral absorption model to separate total absorption (without water) into absorption by phytoplankton, detritus, and gelbstoff. Comparison of model results with *in vivo* absorption data during 2 days at 37 and 52 m reveal that the model successfully determined the spectral shape of each component, with correlations that varied from 0.873 to 0.998. The greatest coherence was found in gelbstoff spectra, and the lowest in phytoplankton spectra. Errors associated with the results are attributed to differences in instruments and measurement techniques as well as in model assumptions and model parameter determination. Variability in the magnitudes of total absorption is due primarily to differences in wavelength selection for the zero-scattering correction technique and to spatial variability caused by differences in sampling techniques.

The separated absorption spectra determined for the entire time series at 37-, 52-, and 68-m depths allowed us to examine vertical and temporal variability of particle types and of relative concentrations of each particle type. The partitioned phytoplankton absorption permits us to investigate particular episodic events (e.g., phytoplankton blooms, hurricanes, and storms) and physical–biological coupling as well as to estimate primary productivity in future studies.

The success of the application of a spectral absorption model demonstrates an important advantage of taking *in situ* high-frequency, long-time-series measurements. Ship-based methods for determining absorption by major components require filtering and pigment extraction of discrete bottle samples. These samples are taken at one discrete time and therefore are not capable of resolving processes, e.g., internal waves, tides, wind mixing and advection events, and eddies, on high-frequency time scales or for extended periods. The application of newly developed instrumentation (e.g., WETLabs, Inc., ac-9 and Hi-Star meters) with the spectral model described above along with complementary shipboard data (profiles and bottle samples) can now be used to measure spectral absorption and to partition total absorption into

absorption that is due to water, phytoplankton, detritus, and gelbstoff and to resolve processes on a broad range of spatial and temporal scales.

This study was supported by the U.S. Office of Naval Research as part of the Coastal Mixing and Optics program (grant N00014-96-1-0669). We thank Collin Roesler (University of Connecticut), and Heidi Sosik and Anne Canaday (Woods Hole Oceanographic Institution) for valuable discussions and for sharing their discrete bottle sample data; W. Scott Pegau (Oregon State University) for his ac-9 calibrations and assistance with data analysis; Murray Levine (Oregon State University), who shared the mooring platform with us; Yogi Agrawal and Chuck Pottsmith (Sequoia Scientific, Inc.) for the use of their bottom tripod; Derek Manov, David Sigurdson, and Erin Lutrick for their engineering and technical support; and Barbara Prezelin, Dave Siegel, and Joe McNeil for their assistance with the development of the manuscript.

References

1. J. T. O. Kirk, *Light and Photosynthesis in Aquatic Ecosystems* (Cambridge U. Press, Cambridge, 1994).
2. C. D. Mobley, *Light and Water: Radiative Transfer in Natural Waters* (Academic, San Diego, Calif., 1994).
3. J. R. V. Zaneveld, "A theoretical derivation of the dependence of the remotely sensed reflectance of the ocean on the inherent optical properties," J. Geophys. Res. **100,** 13,135–13,142 (1995).
4. W. S. Pegau, J. S. Cleveland, W. Doss, C. D. Kennedy, R. A. Maffione, J. L. Mueller, R. Stone, C. C. Trees, A. D. Weidemann, W. H. Wells, and J. R. V. Zaneveld, "A comparison of methods for the measurement of the absorption coefficient in natural waters," J. Geophys. Res. **100,** 13,201–13,220 (1995).
5. M. J. Behrenfeld and P. G. Falkowski, "A consumer's guide to phytoplankton primary productivity models," Limnol. Oceanogr. **42,** 1479–1491 (1997).
6. O. Schofield, B. B. Prezelin, R. C. Smith, P. M. Stegmann, N. B. Nelson, M. R. Lewis, and K. S. Baker, "Variability in spectral and nonspectral measurements of photosynthetic light utilization efficiencies," Mar. Ecol. Prog. Ser. **78,** 253–271 (1991).
7. C. S. Roesler, M. J. Perry, and K. L. Carder, "Modeling *in situ* phytoplankton absorption from total absorption spectra in productive inland marine waters," Limnol. Oceanogr. **34,** 1510–1523 (1989).
8. A. Bricaud and D. Stramski, "Spectral absorption coefficients of living phytoplankton and nonalgal biogenous matter: a comparison between the Peru upwelling area and the Sargasso Sea," Limnol. Oceanogr. **35,** 562–582 (1990).
9. E. J. Bruce, M. Borgerson, C. Moore, and A. Weidemann, "HiStar: a spectrophotometer for measuring the absorption and attenuation of natural waters *in-situ* and in the laboratory," in *Ocean Optics XIII*, S. G. Ackleson, ed., Proc. SPIE **2963,** 637–642 (1996).
10. A. A. Petrenko, B. H. Jones, T. D. Dickey, M. LeHaitre, and C. Moore, "Effects of a sewage plume on the biology, optical characteristics, and particle size distributions of coastal waters," J. Geophys. Res. **102,** 25,061–25,071 (1997).
11. T. D. Dickey, "The emergence of concurrent high-resolution physical and bio-optical measurements in the upper ocean and their applications," Rev. Geophys. **29,** 383–413 (1991).
12. T. Dickey, D. Frye, H. Jannasch, E. Boyle, D. Manov, D. Sigurdson, J. McNeil, M. Stramska, A. Michaels, N. Nelson, D. Siegel, G. Chang, J. Wu, and A. Knap, "Initial results from the Bermuda Testbed Mooring Program," Deep-Sea Res. **45,** 771–794 (1998).
13. D. C. Twichell, B. Butman, and R. S. Lewis, "Shallow structure, surficial geology, and the processes currently shaping the bank," in *Georges Bank*, R. H. Backus, ed. (MIT Press, Cambridge, Mass., 1987), pp. 31–37.
14. D. C. Twichell, C. E. McClennen, and B. Butman, "Morphology and processes associated with the accumulation of the fine-grained sediment deposit on the southern New England shelf," J. Sediment. Petrol. **51,** 269–280 (1981).
15. R. Bartz, R. W. Spinrad, and J. C. Kitchen, "A low power, high resolution, *in situ* fluorometer for profiling and moored applications in water," in *Ocean Optics IX*, SPIE **925,** 157–170 (1988).
16. R. Bartz, J. R. V. Zaneveld, and H. Pak, "A transmissometer for profiling and moored observations in water," in *Ocean Optics V*, M. B. White and R. E. Stevenson, eds., Proc. SPIE **160,** 102–108 (1978).
17. C. Moore, J. R. V. Zaneveld, and J. C. Kitchen, "Preliminary results from *in situ* spectral absorption meter data," in *Ocean Optics XI*, G. D. Gilbert, ed., Proc. SPIE **1750,** 330–337 (1992).
18. C. C. Moore and L. Bruce, "ac-9 Protocols," internal tech. rep. (WETLabs, Inc., Philomath, Ore., 1996).
19. R. C. Smith and K. S. Baker, "Optical properties of the clearest of natural waters," Appl. Opt. **20,** 177–184 (1981).
20. B. G. Mitchell, "Algorithms for determining the absorption coefficient for aquatic particulates using the quantitative filter technique," in *Ocean Optics X*, R. Spinrad, ed., Proc. SPIE **1302,** 137–148 (1990).
21. M. Kishino, M. Takahashi, N. Okami, and S. Ichimura, "Estimation of the spectral absorption coefficients of phytoplankton in the sea," Bull. Mar. Sci. **37,** 634–642 (1985).
22. H. Sosik, Biology Department, Woods Hole Oceanographic Institution, Woods Hole, Mass. 20543 (personal communications, 1997).
23. T. D. Dickey, G. C. Chang, Y. C. Agrawal, A. J. Williams, III, and P. S. Hill, "Sediment resuspension in the wakes of hurricanes Edouard and Hortense," Geophys. Res. Lett. **25,** 3133–3136 (1998).
24. W. S. Pegau, College of Oceanic and Atmospheric Sciences, Oregon State University, Corvallis, Ore., 97331 (personal communications, 1996).
25. R. M. Pope and E. S. Fry, "Absorption spectrum (380–700 nm) of pure water. 2. Integrating cavity measurements," Appl. Opt. **37,** 8710–8723 (1997).
26. N. G. Jerlov, *Optical Oceanography* (Elsevier, New York, 1968).
27. J. S. Cleveland, "Regional models for phytoplankton absorption as a function of chlorophyll *a* concentration," J. Geophys. Res. **100,** 13,333–13,344 (1995).
28. W. S. Pegau and J. R. V. Zaneveld, "Temperature-dependent absorption of water in the red and near-infrared portions of the spectrum," Limnol. Oceanogr. **38,** 188–192 (1993).
29. W. S. Pegau, D. Gray, and J. R. V. Zaneveld, "Absorption and attenuation of visible and near-infrared light in water: dependence on temperature and salinity," Appl. Opt. **36,** 6035–6046 (1997).
30. R. R. Bidigare, M. E. Ondrusek, J. H. Morrow, and D. A. Kiefer, "*In vivo* absorption properties of algal pigments," in *Ocean Optics X*, R. Spinrad, ed., Proc. SPIE **1302,** 290–302 (1990).
31. A. Bricaud, C. Roesler, and J. R. V. Zaneveld, "*In situ* methods for measuring the inherent optical properties of ocean waters," Limnol. Oceanogr. **40,** 393–410 (1995).
32. J. A. Barth, D. Bogucki, S. D. Pierce, and P. M. Kosro, "Secondary circulation associated with a shelfbreak front," Geophys. Res. Lett. **25,** 2761–2764 (1998).
33. B. B. Prezelin, University of California at Santa Barbara, Santa Barbara, Calif. 93106 (personal communications, 1998).
34. J. J. Cura, "Phytoplankton," in *Georges Bank*, R. H. Backus, ed. (MIT Press, Cambridge, Mass., 1987), p. 215.